

SynCo: Synthetic Hard Negatives for Contrastive Visual Representation Learning

Nikolaos Giakoumoglou Tania Stathaki
Imperial College London
London, UK, SW7 2AZ

{n.giakoumoglou23, t.stathaki}@imperial.ac.uk

Abstract

Contrastive learning has become a dominant approach in self-supervised visual representation learning, but efficiently leveraging hard negatives, which are samples closely resembling the anchor, remains challenging. We introduce SynCo (**S**ynthetic **n**egatives in **C**ontrastive learning), a novel approach that improves model performance by generating synthetic hard negatives on the representation space. Building on the MoCo framework, SynCo introduces six strategies for creating diverse synthetic hard negatives on-the-fly with minimal computational overhead. SynCo achieves faster training and strong representation learning, surpassing MoCo-v2 by **+0.4%** and MoCHI by **+1.0%** on ImageNet ILSVRC-2012 linear evaluation. It also transfers more effectively to detection tasks achieving strong results on PASCAL VOC detection (57.2% AP) and significantly improving over MoCo-v2 on COCO detection (**+1.0%** AP^{bb}) and instance segmentation (**+0.8%** AP^{msk}). Our synthetic hard negative generation approach significantly enhances visual representations learned through self-supervised contrastive learning¹.

1. Introduction

Contrastive learning has emerged as a prominent approach in self-supervised learning, significantly advancing representation learning from unlabeled data. This technique, which discriminates between similar and dissimilar data pairs, has shown promise in visual representation tasks. Seminal works such as SimCLR [12] and MoCo [25] established instance discrimination as a pretext task. These methods generate multiple views of the same data point through augmentation, training the model to minimize the distance between positive pairs (augmented views of the same instance) while maximizing it for negative pairs (views of different instances).

Despite its effectiveness, instance discrimination faces challenges. A key limitation is the need for numerous nega-

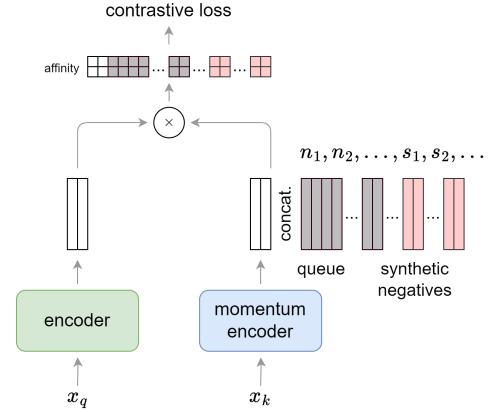


Figure 1. SynCo extends MoCo [14, 25] by introducing synthetic hard negatives generated on-the-fly from a memory queue. The process begins with two augmented views of an image, x_q and x_k , processed by an encoder and a momentum encoder, respectively, producing feature vectors q and k . The memory queue holds negative samples n_1, n_2, \dots , which are concatenated with synthetic hard negatives s_1, s_2, \dots generated using the SynCo strategies. These combined negatives are used to compute the affinity matrix, which, together with the positive pair (query q and key k), contributes to the InfoNCE loss calculation.

tive samples, often leading to increased computational costs. For example, SimCLR requires large batch sizes for sufficient negatives [12]. While approaches like MoCo address some issues through dynamic queues and momentum encoders [14, 25], they still face challenges in selecting and maintaining high-quality hard negatives. Some variations, like SimCo [60], take a different approach by removing both the momentum encoder and queue in favor of a dual temperature mechanism that modulates positive and negative sample distances differently in the InfoNCE loss.

Recent studies have highlighted the importance of carefully crafted data augmentations in learning robust representations [4, 12, 17, 39, 41, 44, 50]. These transformations likely provide more diverse, challenging copies of images, increasing the difficulty of the self-supervised task. This

¹Code is available at <https://github.com/giakoumoglou/synco>.

self-supervised task is a pretext problem (e.g., predicting image rotations [20] or solving jigsaw puzzles [37]) designed to induce learning of generalizable features without explicit labels. Moreover, techniques that combine data at the pixel level [58, 61] or at the feature level [48] have proven effective in helping models learn more resilient features, leading to improvements in both fully supervised and semi-supervised tasks.

The concept of challenging negative samples has been explored as a way to enhance contrastive learning models. These samples, which lie close to the decision boundary, are crucial for refining the model’s discriminative abilities. Recent work like MoCHI [28] has shown improvements by incorporating harder negatives. However, while the potential of hard negatives is clear, recent trends in AI have shifted focus toward large-scale foundation models [2, 8], leaving this promising direction relatively unexplored. Yet, as Yann LeCun observed, *“if AI is a cake, self-supervised learning is the bulk of the cake”*. We argue that revisiting and modernizing self-supervised approaches, particularly through innovative hard negative strategies, remains crucial for advancing AI systems.

In this paper, we present SynCo (Synthetic *negatives* in Contrastive learning), a novel approach to contrastive learning that leverages synthetic hard negatives to enhance the learning process. Building on the foundations of MoCo, SynCo introduces six distinct strategies for generating synthetic hard negatives, each designed to provide diverse and challenging contrasts to the model. These strategies include: interpolated negatives; extrapolated negatives; mixup negatives; noise-injected negatives; perturbed negatives; and adversarial negatives. By incorporating these synthetic samples, SynCo aims to push the boundaries of contrastive learning, improving both the efficiency and effectiveness of the training process.

The main **contributions** of our work are as follows:

- We introduce SynCo, a contrastive learning framework that improves representation learning by leveraging synthetic hard negatives. SynCo enhances model discriminative capabilities by generating challenging negatives on-the-fly from a memory queue, using six distinct strategies targeting different aspects of the feature space. This process improves performance without significant computational increases, achieving faster training and stronger representation learning.
- We empirically show improved downstream performance on ImageNet ILSVRC-2012 by incorporating synthetic hard negatives, demonstrating improvements in both linear evaluation and semi-supervised learning tasks.
- We show that SynCo learns stronger representations by measuring their transfer learning capabilities COCO and PASCAL VOC detection, where it outperforms both the supervised baseline and MoCo.

2. Related Work

2.1. Contrastive Learning

Recent contrastive learning methods like SimCLR [12], BYOL [21]), and SwAV [10] focus on instance discrimination as a pretext task, treating each image as its own class. The core principle involves bringing an anchor and a “positive” sample closer in the representation space while pushing the anchor away from “negative” samples [29]. Positive pairs are typically created through multiple views of each data point [44], using techniques such as color decomposition [43], random augmentation [12, 25], image patches [47], or student-teacher model representations [11, 21, 38]. The common training objective, based on InfoNCE [47] or its variants [12, 17, 46, 57], aims to maximize mutual information [3, 26], necessitating numerous negative pairs. While some approaches like SimCLR use large batch sizes [12] to address this, others like MoCo [14, 25], PIRL [35], and InstDis [53] employ memory structures. Recent advancements explore strategies such as invariance regularizers [36], dataset-derived positives [17], and unified contrastive formulas [42]. Some methods like SimSiam and BYOL eliminate negative samples through asymmetric Siamese structures or normalization [11, 13, 21, 38], while others like Barlow Twins prevent model collapse via redundancy reduction [5, 59] or regularization [6, 7, 63]. Approaches such as LA [64] and PCL [30] address the false-negative pair issue, while DCL [57] further improves representation learning by separating the learning of features and metrics into two distinct phases. Recent work has further refined these approaches, with methods like EqCo [62] establishing equivalences between various components of contrastive learning, and SemPPL [9] leveraging pseudo-labels to guide representation learning.

2.2. Hard Negatives

Hard negatives are critical in contrastive learning as they improve the quality of visual representations by helping to define the representation space more effectively. These challenging yet relevant samples are harder to distinguish from the anchor point, enabling the model to better differentiate between similar features. The use of hard negatives involves selecting samples that are similar to positive samples but different enough to aid in learning distinctive features. Dynamic sampling of hard negatives during training prevents the model from easily minimizing the loss, enhancing its learning capabilities [12, 25]. Various approaches have been proposed to leverage hard negatives effectively. For instance, MoCo [25] utilizes a dynamic queue and momentum-based encoder updates to maintain fresh and challenging negatives throughout training. Other methods, such as SimCLR [12] and InfoMin [44], suggest adjusting the difficulty of negative samples by varying data augmentation techniques. This

progressive increase in task difficulty benefits the training process. Building on these ideas, MoCHI [28] has explored integrating hard negative mixing into existing frameworks to further improve performance. By employing these methods, models become more adept at handling detailed and complex tasks, ensuring each negative sample significantly contributes to optimizing learning outcomes and boosting overall model effectiveness.

3. Preliminaries

3.1. Contrastive Learning

Contrastive learning seeks to differentiate between similar and dissimilar data pairs, often treated as a dictionary look-up where representations are optimized to align positively paired data through contrastive loss in the representation space [25]. Given an image x , and a distribution of image augmentation \mathcal{T} , we create two augmented views of the same image using the transformation $t_q, t_k \sim \mathcal{T}$, i.e., $x_q = t_q(x)$ and $x_k = t_k(x)$. Two encoders, f_q and f_k , namely the query and key encoders, generate the vectors $\mathbf{q} = f_q(x_q)$ and $\mathbf{k} = f_k(x_k)$, respectively. The learning objective minimizes a contrastive loss using the InfoNCE criterion [47]:

$$\mathcal{L}(\mathbf{q}, \mathbf{k}, \mathcal{Q}) = -\log \frac{\exp(\mathbf{q}^T \cdot \mathbf{k} / \tau)}{\exp(\mathbf{q}^T \cdot \mathbf{k} / \tau) + \sum_{\mathbf{n} \in \mathcal{Q}} \exp(\mathbf{q}^T \cdot \mathbf{n} / \tau)} \quad (1)$$

Here, \mathbf{k} is f_k 's output from the same augmented image as \mathbf{q} , and $\mathcal{Q} = \{\mathbf{n}_1, \mathbf{n}_2, \dots, \mathbf{n}_K\}$ includes outputs from different images, representing negative samples of size K . The temperature parameter τ adjusts scaling for the ℓ_2 -normalized vectors \mathbf{q} and \mathbf{k} . The key encoder f_k can be updated in two ways. In the synchronized update approach, f_k is updated synchronously with f_q , maintaining identical weights throughout training [12]. Alternatively, a momentum update scheme can be employed, where f_k is updated using the equation: $\theta_k \leftarrow m \cdot \theta_k + (1 - m) \cdot \theta_q$ [25]. Here, θ_k and θ_q are the parameters of f_k and f_q respectively, and $m \in [0, 1]$ is the momentum coefficient. This momentum approach allows f_k to evolve more slowly, providing more consistent negative samples over time and potentially stabilizing the learning process. The memory bank \mathcal{Q} can be defined in various ways, such as an external memory of all dataset images [35, 43, 53], a queue of recent batches [25], or the current minibatch [12]. Recent analysis [33] has shown that the projection head's normalization significantly influences training dynamics and representation quality.

The gradient of the contrastive loss in Equation (1) with respect to the query \mathbf{q} is given by:

$$\frac{\partial \mathcal{L}(\mathbf{q}, \mathbf{k}, \mathcal{Q})}{\partial \mathbf{q}} = -\frac{1}{\tau} \left((1 - p_k) \cdot \mathbf{k} - \sum_{\mathbf{n} \in \mathcal{Q}} p_n \cdot \mathbf{n} \right) \quad (2)$$

where

$$p_{z_i} = \frac{\exp(\mathbf{q}^T \cdot \mathbf{z}_i / \tau)}{\sum_{j \in Z} \exp(\mathbf{q}^T \cdot \mathbf{z}_j / \tau)} \quad (3)$$

with \mathbf{z}_i being a member of the set $\mathcal{Q} \cup \{\mathbf{k}\}$. The positive and negative logits contribute to the loss similarly to a $(K + 1)$ -way cross-entropy classification, with the key logit representing the query's latent class [1].

3.2. Understanding Hard Negatives

The effectiveness of contrastive learning approaches hinges critically on the utilization of hard negatives [1, 22, 27, 28, 34, 53]. Current approaches face significant challenges in efficiently leveraging these hard negatives. Sampling from within the same batch necessitates larger batch sizes [12, 15], potentially straining computational resources. Conversely, maintaining a memory bank containing representations of the entire dataset incurs substantial computational overhead in keeping the memory up-to-date [14, 25, 35, 53]. These limitations underscore the need for more efficient strategies to generate and utilize hard negatives in contrastive learning frameworks.

Hardness of negatives. The "hardness" of negative samples, defined by their similarity to positive samples in the representation space, determines how challenging they are for the model to differentiate, directly impacting the effectiveness of the contrastive learning process. Figure 2 illustrates the evolution of negative sample hardness during MoCo-v2 training on ImageNet-100. The plot depicts the top 1024 matching probabilities p_{z_i} across different training epochs. Initially, the distribution of these probabilities is relatively uniform. However, as training progresses, a clear trend emerges: fewer negatives contribute significantly to the loss function. This observation suggests that the model rapidly learns to distinguish most negatives, leaving only a small subset that remains challenging. Such a phenomenon underscores the importance of maintaining a diverse pool of hard negatives throughout the training process to sustain effective learning [28].

Difficulty of the proxy task. The difficulty of the proxy task in contrastive learning, typically defined by the self-supervised objective, significantly influences the quality of learned representations. Figure 3 compares the proxy task performance of MoCo and MoCo-v2 on ImageNet-100, measured by the percentage of queries where the key ranks above all negatives. Notably, MoCo-v2, which employs more aggressive augmentations, exhibits lower proxy task performance compared to MoCo, indicating a more challenging learning objective. Paradoxically, this increased difficulty correlates with improved performance on downstream tasks

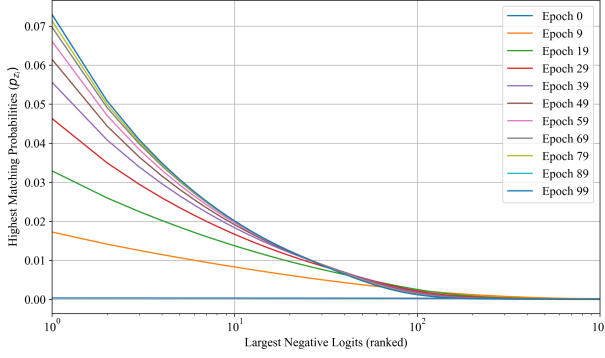


Figure 2. Histogram of the top 1024 matching probabilities p_{z_i} , $z_i \in \mathcal{Q}$ for MoCo-v2, over various epochs. Logits are organized in descending order, and each line indicates the mean matching probability across all queries [28].

such as linear classification [28]. This counterintuitive relationship between proxy task difficulty and downstream performance suggests that more challenging self-supervised objectives can lead to the learning of more robust and transferable representations, motivating the development of strategies to dynamically modulate task difficulty during training.

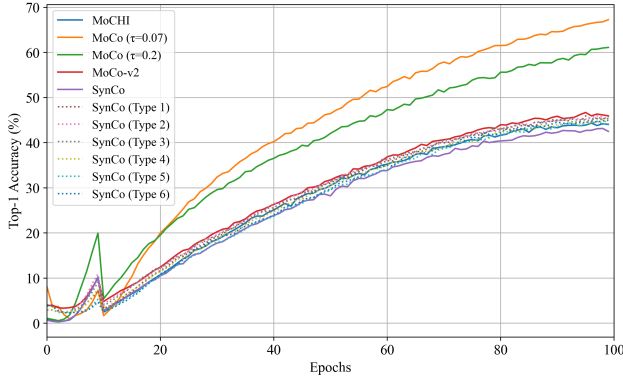


Figure 3. Performance comparison of MoCo, MoCo-v2, MoCHI, and SynCo (under various configurations) on ImageNet-100 in terms of accuracy on the proxy task (percentage of queries where the key is ranked higher than all negatives).

4. Synthetic Hard Negatives in Contrastive Learning

In this section, we present an approach for generating synthetic hard negatives in the representation space using six distinct strategies. Building on MoCHI’s foundation of interpolation and mixup strategies, we propose *four* additional methods for generating synthetic hard negatives to explore complementary aspects of the representation space. We refer to our proposed approach as SynCo (“Synthetic *n*egatives in

Contrastive learning”).

4.1. Generating Synthetic Hard Negatives

Let \mathbf{q} represent the query image, \mathbf{k} its corresponding key, and $\mathbf{n} \in \mathcal{Q}$ denote the negative features from a memory structure of size K . The loss associated with the query is computed using the logits $\ell(\mathbf{z}_i) = \mathbf{q}^T \cdot \mathbf{z}_i / \tau$, which are processed through a softmax function. We define $\hat{\mathcal{Q}} = \mathbf{n}_1, \mathbf{n}_2, \dots, \mathbf{n}_K$ as the ordered set of all negative features, where $\ell(\mathbf{n}_i) > \ell(\mathbf{n}_j)$ for all $i < j$, implying that the negative features are sorted based on decreasing similarity to the query. The most challenging negatives are selected by truncating the ordered set $\hat{\mathcal{Q}}$, retaining only the first $N < K$ elements, denoted as $\hat{\mathcal{Q}}^N$.

Interpolated synthetic negatives (type 1). Building on MoCHI’s [28] foundation, our first strategy creates synthetic negatives through controlled interpolation between samples. This approach aims to generate features that lie in meaningful regions of the representation space between the query and existing hard negatives. For each query \mathbf{q} , we propose to generate N_1 synthetic hard negative features by mixing the query \mathbf{q} with a randomly chosen feature from the N hardest negatives in $\hat{\mathcal{Q}}^N$. Let $S^1 = \{\mathbf{s}_1^1, \mathbf{s}_2^1, \dots, \mathbf{s}_{N_1}^1\}$ be the set of synthetic negatives to be generated. Then a synthetic negative feature $\mathbf{s}_k^1 \in S^1$ would be given by:

$$\mathbf{s}_k^1 = \alpha_k \cdot \mathbf{q} + (1 - \alpha_k) \cdot \mathbf{n}_i, \quad \alpha_k \in (0, \alpha_{\max}) \quad (4)$$

where $\mathbf{n}_i \in \hat{\mathcal{Q}}^N$ and α_k is randomly sampled from a uniform distribution in the range $(0, \alpha_{\max})$. The resulting synthetic hard negatives are then normalized and added to the set of negative logits for the query. Interpolation creates a synthetic embedding that lies between the query and the negative in the representation space. We set $\alpha_{\max} = 0.5$ to guarantee that the contribution of the query is always less than that of the negative. This is similar to the hardest negatives (type 2) of MoCHI [28].

Extrapolated synthetic negatives (type 2). As a natural extension of interpolation, we propose extrapolation to explore the “opposite” direction in feature space. While this approach operates further from the decision boundary, we carefully control the exploration through coefficients to maintain an appropriate level of task difficulty. For each query \mathbf{q} , we propose to generate N_2 hard negative features by extrapolating beyond the query embedding in the direction of the hardest negative features. Similar to the interpolated method, we use a randomly chosen feature from the N hardest negatives in $\hat{\mathcal{Q}}^N$. Let $S^2 = \{\mathbf{s}_1^2, \mathbf{s}_2^2, \dots, \mathbf{s}_{N_2}^2\}$ be the set of synthetic negatives to be generated. Then a synthetic negative feature $\mathbf{s}_k^2 \in S^2$ would be given by:

$$\mathbf{s}_k^2 = \mathbf{n}_i + \beta_k \cdot (\mathbf{n}_i - \mathbf{q}), \quad \beta_k \in (1, \beta_{\max}) \quad (5)$$

where $\mathbf{n}_i \in \hat{\mathcal{Q}}^N$ and β_k is randomly sampled from a uniform distribution in the range $(1, \beta_{\max})$. These synthetic features are also normalized and used to enhance the negative logits. Extrapolation generates a synthetic embedding that lies beyond the query embedding in the direction of the hardest negative. We choose $\beta_{\max} = 1.5$.

Mixup synthetic negatives (type 3). Following MoCHI’s [28] effective strategy of mixing hard negatives, we incorporate their approach of combining pairs of challenging examples. For each query \mathbf{q} , we propose to generate N_3 hard negative features by combining pairs of the N hardest existing negative features in $\hat{\mathcal{Q}}^N$. Let $S^3 = \{\mathbf{s}_1^3, \mathbf{s}_2^3, \dots, \mathbf{s}_{N_3}^3\}$ be the set of synthetic negatives to be generated. Then a synthetic negative feature $\mathbf{s}_k^3 \in S^3$ would be given by:

$$\mathbf{s}_k^3 = \gamma_k \cdot \mathbf{n}_i + (1 - \gamma_k) \cdot \mathbf{n}_j, \quad \gamma_k \in (0, 1) \quad (6)$$

where $\mathbf{n}_i, \mathbf{n}_j \in \hat{\mathcal{Q}}^N$ and γ_k is randomly sampled from a uniform distribution in the range $(0, 1)$. The resulting synthetic hard negatives are then normalized and added to the set of negative logits for the query. Mixup combines pairs of the hardest existing negative features to create a synthetic embedding that represents a blend of challenging cases. This is similar to the hard negatives (type 1) of MoCHI [28].

Noise-injected synthetic negatives (type 4). To prevent overfitting to specific negative patterns while maintaining the essential characteristics of hard negatives, we introduce controlled stochasticity through noise injection. For each query \mathbf{q} , we propose to generate N_4 hard negative features by adding Gaussian noise to the hardest negative features. Using the top N hardest negatives $\hat{\mathcal{Q}}^N$, let $S^4 = \{\mathbf{s}_1^4, \mathbf{s}_2^4, \dots, \mathbf{s}_{N_4}^4\}$ be the set of synthetic negatives to be generated. Then a synthetic negative feature $\mathbf{s}_k^4 \in S^4$ would be given by:

$$\mathbf{s}_k^4 = \mathbf{n}_i + \mathcal{N}(\mathbf{0}, \sigma^2 \cdot \mathbf{I}) \quad (7)$$

where $\mathbf{n}_i \in \hat{\mathcal{Q}}^N$ and $\mathcal{N}(\mathbf{0}, \sigma^2 \cdot \mathbf{I})$ represents Gaussian noise with standard deviation σ (where \mathbf{I} is the identity matrix). The noisy negatives are normalized before being used in the loss calculation. Noise injection adds Gaussian noise to the hardest negative features, resulting in a synthetic embedding with added randomness.

Perturbed synthetic negatives (type 5). Drawing inspiration from adversarial training [32], we introduce perturbed synthetic negatives that use gradient-based perturbations with variable magnitudes. For each query \mathbf{q} , we propose

to generate N_5 hard negative features by perturbing the embeddings of the hardest negative features. Given the top N hardest negatives $\hat{\mathcal{Q}}^N$, let $S^5 = \{\mathbf{s}_1^5, \mathbf{s}_2^5, \dots, \mathbf{s}_{N_5}^5\}$ be the set of synthetic negatives to be generated. Then a synthetic negative feature $\mathbf{s}_k^5 \in S^5$ would be given by:

$$\mathbf{s}_k^5 = \mathbf{n}_i + \delta \cdot \nabla_{\mathbf{n}_i} \text{sim}(\mathbf{q}, \mathbf{n}_i) \quad (8)$$

where $\mathbf{n}_i \in \hat{\mathcal{Q}}^N$ and $\text{sim}(\cdot, \cdot)$ is the similarity function and δ controls the perturbation magnitude. The perturbed embeddings are then normalized and added to the negative logits. Perturbation modifies the embeddings of the hardest negative features based on the gradient of the similarity function, creating synthetic negatives that are slightly adjusted to be more challenging for the model. This approach offers greater flexibility than fixed interpolation, as it generalizes to arbitrary similarity functions and can generate negatives of varying hardness.

Adversarial synthetic negatives (type 6). While similar in concept to type 5, adversarial synthetic negatives differ fundamentally in their gradient scaling approach. For each query \mathbf{q} , we propose to generate N_6 hard negative features by applying adversarial perturbations to the hardest negative features to maximize their similarity to the query embeddings. Using the top N hardest negatives $\hat{\mathcal{Q}}^N$, let $S^6 = \{\mathbf{s}_1^6, \mathbf{s}_2^6, \dots, \mathbf{s}_{N_6}^6\}$ be the set of synthetic negatives to be generated. Then a synthetic negative feature $\mathbf{s}_k^6 \in S^6$ would be given by:

$$\mathbf{s}_k^6 = \mathbf{n}_i + \eta \cdot \text{sign}(\nabla_{\mathbf{n}_i} \text{sim}(\mathbf{q}, \mathbf{n}_i)) \quad (9)$$

where $\mathbf{n}_i \in \hat{\mathcal{Q}}^N$ and η controls the perturbation magnitude. The perturbed embeddings are normalized and added to the negative logits. Adversarial hard negatives apply adversarial perturbations to the hardest negative features, specifically altering them to maximize their similarity to the query embeddings, thereby producing the most challenging contrasts. Where type 5 allows variable perturbation sizes, type 6 enforces unit magnitude through the sign function, creating consistently challenging contrasts.

4.2. Integrating Synthetic Hard Negatives into the Contrastive Loss

The synthetic hard negatives generated are integrated into the contrastive learning process by modifying the InfoNCE loss. Let $\mathcal{S} = \bigcup_{i=1}^6 S^i$ represent the concatenation of all synthetic hard negatives, where S^i is the set of synthetic negatives generated by the i -th strategy. This combined set of synthetic negatives augments the original negatives \mathcal{Q} , providing a more diverse and challenging set of contrasts for the query. The modified InfoNCE loss is given by:

$$\mathcal{L}(\mathbf{q}, \mathbf{k}, \mathcal{Q}, \mathcal{S}) = -\log \frac{\exp(\mathbf{q}^T \cdot \mathbf{k} / \tau)}{\exp(\mathbf{q}^T \cdot \mathbf{k} / \tau) + Z} \quad (10)$$

where Z represents the negative samples:

$$Z = \underbrace{\sum_{\mathbf{n} \in \mathcal{Q}} \exp(\mathbf{q}^T \cdot \mathbf{n} / \tau)}_{\text{memory-based negatives}} + \underbrace{\sum_{\mathbf{s} \in \mathcal{S}} \exp(\mathbf{q}^T \cdot \mathbf{s} / \tau)}_{\text{synthetic negatives}} \quad (11)$$

Here, τ is the temperature parameter, \mathcal{Q} is the set of original memory-based negatives, and \mathcal{S} is the set of synthetic hard negatives. By incorporating both real and synthetic negatives, the model is exposed to a wider variety of challenging examples, which encourages learning more robust and generalizable representations. The overall computational overhead of SynCo is roughly equivalent to increasing the queue/memory by $\sum_{i=1}^6 N_i \ll K$, along with the additional yet negligible cost of generating the synthetic negatives.

5. Experiments

5.1. Implementation Details

We pretrain SynCo on ImageNet ILSVRC-2012 [16] and its smaller ImageNet-100 subset [43] using a ResNet-50 [23] encoder. Our implementation builds upon MoCo-v2 [14]; thus it’s only *fair* to compare with MoCo-based methods [14, 28, 30, 57] that share similar architectural choices and training procedures. For training, unless stated otherwise, we use $K = 65\text{k}$. For SynCo, we also have a warm-up of 10 epochs, i.e. for the first epochs we do not synthesize hard negatives. We set SynCo’s hyperparameters σ , δ , and η to 0.01. For hard negative generation, we use the top $N = 1024$ hardest negatives, with $N_1 = N_2 = N_3 = 256$ and $N_4 = N_5 = N_6 = 64$. For ImageNet linear evaluation, we train a linear classifier on frozen features for 100 epochs, using a batch size of 256 and a cosine learning rate schedule. Initial learning rates are set to 30.0 for ImageNet and 10.0 for ImageNet-100. To evaluate transfer learning, we apply SynCo to object detection tasks. For PASCAL VOC [18], we fine-tune a Faster R-CNN [40] on `trainval07+12` and test on `test2007`. For COCO [31], we use a Mask R-CNN [24], fine-tuning on `train2017` and evaluating on `val2017`. We employ Detectron2 [52] and report standard AP metrics, following [25] *without* additional hyperparameter tuning. Detailed implementation details along ablations are provided in the supplementary material.

5.2. Linear Evaluation on ImageNet

We evaluate the SynCo representation by training a linear classifier on top of the frozen features pretrained on ImageNet. With 200 epochs pretraining (Table 1), SynCo obtains $67.9\% \pm 0.16\%$ top-1 accuracy and $88.0\% \pm 0.05\%$

top-5 accuracy, showing strong improvements over MoCo-based methods (**+0.4%** over MoCo-v2, **+1.0%** over MoCHI, **+0.3%** over PCL-v2 and DCL). While MoCHI’s hard negative generation leads to lower performance than MoCo-v2, our synthetic hard negatives achieve consistent gains. When training for 800 epochs (Table 2), SynCo reaches 70.7% top-1 accuracy (**+2.0%** over MoCHI) and 89.8% top-5 accuracy. However, at 800 epochs, it does not surpass MoCo-v2, similar to what is also observed with MoCHI, likely due to an overly hard proxy task [28].

Table 1. Top-1 and top-5 accuracies (in %) under linear evaluation on ImageNet ILSVRC-2012 with 200 epochs of pretraining using ResNet-50. Results for SynCo are given as max/avg. over 3 runs.

Method	Top-1	Top-5
<i>Supervised</i>		
PIRL [35]	63.6	-
InfoMin [44]	70.1	89.4
SimSiam [13]	68.1	-
SimCLR-v2 + DCL [57]	65.8	-
<i>MoCo-based</i>		
MoCo [25]	60.7	-
MoCo-v2 [14]	67.5	90.1
PCL-v2 [30]	67.6	-
MoCo-v2 + DCL [57]	67.6	-
MoCHI [28]	66.9	-
SynCo (ours)	68.1/67.9	88.0

Table 2. Top-1 and top-5 accuracies (in %) under linear evaluation on ImageNet ILSVRC-2012 for models trained with extended epochs using ResNet-50. Results for SynCo are based on 1 run.

Method	Epochs	Top-1	Top-5
PIRL [35]	800	63.6	-
InfoMin [44]	800	73.0	91.1
SimSiam [13]	800	68.1	-
SimCLR [12]	1000	69.3	-
BT [59]	1000	73.2	91.0
BYOL [21]	1000	74.3	91.6
SwAV [21]	800	75.3	-
<i>MoCo-based</i>			
MoCo-v2 [14]	800	71.1	90.1
MoCHI [28]	800	68.7	-
SynCo (ours)	800	70.7	89.8

5.3. Semi-supervised Training on ImageNet

We evaluate SynCo in a semi-supervised setting using 1% and 10% of labeled ImageNet data. Results in Table 3 show that with 1% labels, SynCo achieves $50.8\% \pm 0.21\%$ top-1

accuracy (+25.4% over supervised baseline, +2.6% over MoCo-v2, +2.5% over SimCLR) and $77.5\% \pm 0.12\%$ top-5 accuracy. With 10% labels, it reaches $66.6\% \pm 0.19\%$ top-1 (+10.2% over supervised, +0.5% over MoCo-v2, +1.0% over SimCLR) and $88.0\% \pm 0.10\%$ top-5 accuracy, despite using fewer training epochs than SimCLR.

Table 3. Semi-supervised learning on ImageNet ILSVRC-2012 with 1% and 10% training examples using ResNet-50. Results for SynCo are averaged over 3 runs.

Method	Epochs	Top-1		Top-5	
		1%	10%	1%	10%
<i>Supervised</i>		25.4	56.4	48.4	80.4
PIRL [35]	800	30.7	60.4	57.2	83.8
SimCLR [12]	1000	48.3	65.6	75.5	87.8
BT [59]	1000	55.0	69.7	79.2	89.3
BYOL [21]	1000	53.2	68.8	78.4	89.0
SwAV [10]	800	53.9	70.2	78.5	89.9
<i>MoCo-based</i>					
MoCo-v2 (repr.)	800	48.2	66.1	75.8	87.6
MoCHI (repr.)	800	50.4	65.7	76.2	87.2
SynCo (ours)	800	50.8	66.6	77.5	88.0

5.4. Transferring to Detection

We evaluate the SynCo representation, pretrained for 200 epochs, by applying it to detection tasks. Table 4 shows that on PASCAL VOC, SynCo achieves strong results (57.2 AP) comparable to MoCHI (57.5 AP), while significantly outperforming the supervised baseline (+3.7 AP). On the more challenging COCO dataset with $1 \times$ schedule, SynCo shows consistent improvements over the supervised baseline (AP^{bb} +1.7, AP^{msk} +1.6) and MoCo-v2 (AP^{bb} +1.0, AP^{msk} +0.8). SynCo achieves competitive performance with detection-specific methods, showing comparable results to DetCo (39.8 vs 39.9 AP^{bb}) and InsLoc (39.5 vs 39.9 AP^{bb}), despite using a general contrastive learning framework.

6. Discussion

6.1. Is the Proxy Task More Difficult?

Figure 3 depicts the proxy task performance for different configurations of SynCo. We observe that incorporating synthetic negatives leads to faster learning and improved performance. Each type of synthetic negative accelerates learning compared to the MoCo-v2 baseline, with the full SynCo configuration showing the most significant improvement (see supplementary material) and the lowest final proxy task performance. This indicates that SynCo presents the most challenging proxy task. This is evidenced by $\max \ell(s_k^i) > \max \ell(n_j)$, where $s_k^i \in S^i$ are synthetic negatives and $n_j \in \mathcal{Q}_N$ are original negatives. Through SynCo,

we modulate proxy task difficulty via synthetic negatives, pushing the model to learn more robust features.

6.2. Evaluating the Usage of the Representation Space

To assess learned representations, we employ alignment and uniformity metrics proposed by [49]. These metrics provide insights into representation space utilization, with alignment quantifying the grouping of similar samples and uniformity measuring representation spread across the hypersphere. Figure 4 presents results for various models using features from the ImageNet-100 validation set. Our findings demonstrate that SynCo significantly enhances the uniformity of representations compared to MoCo-v2 and MoCHI, demonstrating improved utilization of the representation space in the proxy task. Furthermore, the incorporation of synthetic negatives (types 1 to 6) leads to improved alignment. These results suggest that SynCo’s approach to synthetic negative generation and contrastive learning yields stronger and more well-distributed feature representations.

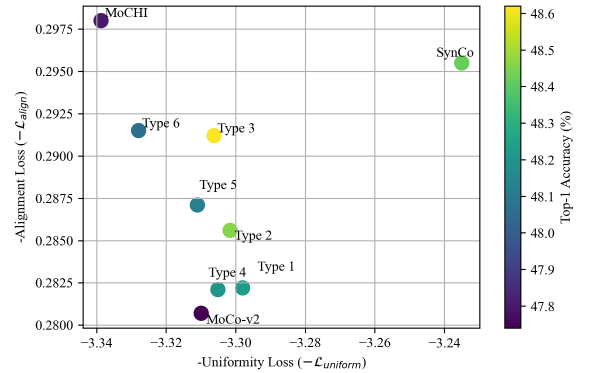


Figure 4. Performance comparison of MoCo-v2, MoCHI, and SynCo (under various configurations) on ImageNet-100 in terms of alignment and uniformity metrics. The x-axis and y-axis represent $-\mathcal{L}_{\text{uniform}}$ and $-\mathcal{L}_{\text{align}}$, respectively. The model with the highest performance is located in the upper-right corner of the chart.

6.3. Class Concentration Analysis

Figure 5 shows the distribution of ratios between inter-class and intra-class ℓ_2 -distances for representations learned by various MoCo-based contrastive learning methods on the ImageNet validation set. A higher mean ratio indicates that representations are better concentrated within classes while maintaining greater separation between classes, reflecting improved linear separability (aligned with Fisher’s linear discriminant analysis principles [19]). After 800 training epochs, SynCo achieves a mean ratio of 1.384, significantly surpassing MoCo-v2 at 800 epochs (1.146) and PCL-v2 at 200 epochs (0.988).

Table 4. Transfer learning on PASCAL VOC and COCO using R50-C4. For COCO experiments, both $1\times$ and $2\times$ training schedules are used. We report AP, AP₅₀, and AP₇₅, which are standard COCO metrics. *bb* denotes bounding box detection, and *msk* denotes instance segmentation. Results for SynCo are averaged over 3 runs.

Method	VOC07+12			COCO $1\times$ schedule						COCO $2\times$ schedule					
	AP	AP ₅₀	AP ₇₅	AP ^{bb}	AP ₅₀ ^{bb}	AP ₇₅ ^{bb}	AP ^{msk}	AP ₅₀ ^{msk}	AP ₇₅ ^{msk}	AP ^{bb}	AP ₅₀ ^{bb}	AP ₇₅ ^{bb}	AP ^{msk}	AP ₅₀ ^{msk}	AP ₇₅ ^{msk}
<i>Supervised</i>	53.5	81.3	58.8	38.2	58.2	41.2	33.3	54.7	35.2	40.0	59.9	43.1	34.7	56.5	36.9
<i>Random init</i>	33.8	60.2	33.1	26.4	44.0	27.8	29.3	46.9	30.8	35.6	54.6	38.2	31.4	51.5	33.5
InstDis [53]	55.2	80.9	61.2	37.7	57.0	40.9	33.0	54.1	35.2	-	-	-	-	-	-
PIRL [35]	55.5	81.0	61.3	37.4	56.5	40.2	32.7	53.4	34.7	-	-	-	-	-	-
InfoMin [44]	57.6	82.7	64.6	39.0	58.5	42.0	34.1	55.2	36.3	41.3	61.2	45.0	36.0	57.9	38.3
SimSiam [13]	57.0	82.4	63.7	39.2	59.3	42.1	34.4	56.0	36.7	-	-	-	-	-	-
BYOL [21] [†]	51.9	81.0	56.5	-	-	-	-	-	-	40.3	60.5	43.9	35.1	56.8	37.3
SwAV [10] [‡]	56.1	82.6	62.7	38.4	58.6	41.3	33.8	55.2	35.9	-	-	-	-	-	-
BT [59] [‡]	56.8	82.6	63.4	39.2	59.0	42.5	34.3	56.0	36.5	-	-	-	-	-	-
SimCLR [12] [‡]	56.3	81.9	62.5	-	-	-	-	-	-	40.3	60.5	43.9	35.1	56.8	37.3
<i>Detection-specific</i>															
SoCo [51] [†]	59.1	83.4	65.6	40.4	60.4	43.7	34.9	56.8	37.0	41.1	61.0	44.4	35.6	57.5	38.0
InsLoc [56]	57.9	82.9	64.9	39.5	59.1	42.7	34.5	56.0	36.8	41.4	60.9	45.0	35.9	57.6	38.4
DetCo [55]	57.8	82.6	64.2	39.8	59.7	43.0	34.7	56.3	36.7	41.3	61.2	45.0	35.8	57.9	38.2
ReSim [54]	58.7	83.1	66.3	39.7	59.0	43.0	34.6	55.9	37.1	-	-	-	-	-	-
<i>MoCo-based</i>															
MoCo [25]	55.9	81.5	62.6	38.5	58.3	41.6	33.6	54.8	35.6	40.7	60.5	44.1	35.6	57.4	38.1
MoCo-v2 [14]	57.0	82.4	63.6	38.9	58.6	41.9	34.1	55.5	36.0	40.7	60.5	44.1	35.6	57.4	37.1
MoCHI [28]	57.5	82.7	64.4	39.2	58.9	42.4	34.3	55.5	36.6	-	-	-	-	-	-
SynCo (ours)	57.2	82.6	63.9	39.9	59.6	43.3	34.9	56.5	36.9	41.0	60.6	44.8	35.7	57.4	38.1

[†] Methods trained for extended epochs include BYOL (300), SwAV (800), BT (1000), and SimCLR (1000).

[‡] Methods trained for fewer epochs include SoCo (100).

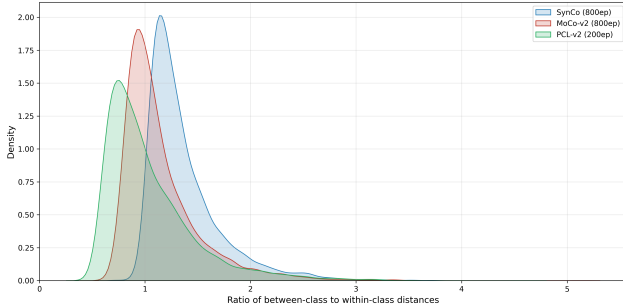


Figure 5. Distribution of the ratio between inter-class and intra-class distances for MoCo-based methods. Higher values indicate better class separation. For clarity, we only show MoCo-v2 [14] (800 epochs), PCL-v2 [30] (200 epochs), and SynCo (800 epochs).

7. Conclusion

This paper introduces SynCo, a novel contrastive learning approach leveraging synthetic hard negatives to enhance visual representation learning. By generating diverse and challenging negatives on-the-fly, SynCo overcomes the limitations of maintaining an effective hard negative pool throughout training. Comprehensive experiments demonstrate that

SynCo accelerates learning and produces more robust, transferable representations. Its effectiveness is validated across benchmarks, including linear evaluation on ImageNet, semi-supervised learning tasks, and transfer learning to object detection on PASCAL VOC and COCO.

While our experiments primarily employed the MoCo framework for the lower batch size requirements, the proposed hard negative generation strategies are general and applicable to any contrastive learning method that benefits from hard negatives, such as SimCLR [12], CPC [47], PIRL [35], and other approaches [17, 45, 50]. These methods, which utilize the InfoNCE loss function (or its variants [12, 17]) and instance discrimination as the pretext task, gain from SynCo’s enhanced hard negative generation. By introducing synthetic hard negatives, these methods access more challenging, informative contrasts, potentially improving feature representations. Performance could be further improved by dynamically adjusting or stopping hard negative generation in later training stages. Furthermore, SynCo’s applicability extends beyond visual representation learning, offering benefits in domains such as natural language processing, audio processing, and other areas where contrastive learning is relevant.

Broader Impact

The presented research should be categorized as research in the field of unsupervised learning. This work may inspire new algorithms, theoretical, and experimental investigation. The algorithm presented here can be used for many different vision applications and a particular use may have both positive or negative impacts, which is known as the dual use problem. Besides, as vision datasets could be biased, the representation learned by SynCo could be susceptible to replicate these biases.

Acknowledgments

We would like to express our gratitude to Andreas Floros for his valuable feedback, particularly his assistance with equations, notations, and insightful discussions that greatly contributed to this work. We also acknowledge the computational resources and support provided by the Imperial College Research Computing Service (<http://doi.org/10.14469/hpc/2232>), which enabled our experiments.

References

- [1] Sanjeev Arora, Hrishikesh Khandeparkar, Mikhail Khodak, Orestis Plevrakis, and Nikunj Saunshi. A theoretical analysis of contrastive unsupervised representation learning, 2019. 3
- [2] Muhammad Awais, Muzammal Naseer, Salman Khan, Rao Muhammad Anwer, Hisham Cholakkal, Mubarak Shah, Ming-Hsuan Yang, and Fahad Shahbaz Khan. Foundational models defining a new era in vision: A survey and outlook, 2023. 2
- [3] Philip Bachman, R Devon Hjelm, and William Buchwalter. Learning representations by maximizing mutual information across views, 2019. 2
- [4] Randall Balestriero, Mark Ibrahim, Vlad Sobal, Ari Morcos, Shashank Shekhar, Tom Goldstein, Florian Bordes, Adrien Bardes, Gregoire Mialon, Yuandong Tian, Avi Schwarzschild, Andrew Gordon Wilson, Jonas Geiping, Quentin Garrido, Pierre Fernandez, Amir Bar, Hamed Pirsiavash, Yann LeCun, and Micah Goldblum. A cookbook of self-supervised learning, 2023. 1
- [5] Wele Gedara Chaminda Bandara, Celso M. De Melo, and Vishal M. Patel. Guarding barlow twins against overfitting with mixed samples, 2023. 2
- [6] Adrien Bardes, Jean Ponce, and Yann LeCun. Vicreg: Variance-invariance-covariance regularization for self-supervised learning, 2022. 2
- [7] Adrien Bardes, Jean Ponce, and Yann LeCun. Vicregl: Self-supervised learning of local visual features, 2022. 2
- [8] Rishi Bommasani, Drew A. Hudson, Ehsan Adeli, Russ Altman, Simran Arora, Sydney von Arx, Michael S. Bernstein, Jeannette Bohg, Antoine Bosselut, Emma Brunskill, Erik Brynjolfsson, S. Buch, Dallas Card, Rodrigo Castellon, Niladri S. Chatterji, Annie S. Chen, Kathleen A. Creel, Jared Davis, Dora Demszky, Chris Donahue, Moussa Doumboya, Esin Durmus, Stefano Ermon, John Etchemendy, Kawin Ethayarajh, Li Fei-Fei, Chelsea Finn, Trevor Gale, Lauren E. Gillespie, Karan Goel, Noah D. Goodman, Shelby Grossman, Neel Guha, Tatsunori Hashimoto, Peter Henderson, John Hewitt, Daniel E. Ho, Jenny Hong, Kyle Hsu, Jing Huang, Thomas F. Icard, Saahil Jain, Dan Jurafsky, Pratyusha Kalluri, Siddharth Karamcheti, Geoff Keeling, Fereshte Khani, O. Khattab, Pang Wei Koh, Mark S. Krass, Ranjay Krishna, Rohith Kudithipudi, Ananya Kumar, Faisal Ladhak, Mina Lee, Tony Lee, Jure Leskovec, Isabelle Levent, Xiang Lisa Li, Xuechen Li, Tengyu Ma, Ali Malik, Christopher D. Manning, Suvir P. Mirchandani, Eric Mitchell, Zanele Muniyikwa, Suraj Nair, Avani Narayan, Deepak Narayanan, Benjamin Newman, Allen Nie, Juan Carlos Nieves, Hamed Nilforoshan, J. F. Nyarko, Giray Ogut, Laurel Orr, Isabel Papadimitriou, Joon Sung Park, Chris Piech, Eva Portelance, Christopher Potts, Aditi Raghunathan, Robert Reich, Hongyu Ren, Frieda Rong, Yusuf H. Roohani, Camilo Ruiz, Jack Ryan, Christopher R’e, Dorsa Sadigh, Shiori Sagawa, Keshav Santhanam, Andy Shih, Krishna Parasuram Srinivasan, Alex Tamkin, Rohan Taori, Armin W. Thomas, Florian Tramèr, Rose E. Wang, William Wang, Bohan Wu, Jiajun Wu, Yuhuai Wu, Sang Michael Xie, Michihiro Yasunaga, Jiaxuan You, Matei A. Zaharia, Michael Zhang, Tianyi Zhang, Xikun Zhang, Yuhui Zhang, Lucia Zheng, Kaitlyn Zhou, and Percy Liang. On the opportunities and risks of foundation models. *ArXiv*, 2021. 2
- [9] Matko Bošnjak, Pierre H. Richemond, Nenad Tomasev, Florian Strub, Jacob C. Walker, Felix Hill, Lars Holger Buesing, Razvan Pascanu, Charles Blundell, and Jovana Mitrovic. Semppl: Predicting pseudo-labels for better contrastive representations, 2024. 2
- [10] Mathilde Caron, Ishan Misra, Julien Mairal, Priya Goyal, Piotr Bojanowski, and Armand Joulin. Unsupervised learning of visual features by contrasting cluster assignments. In *Advances in Neural Information Processing Systems*, pages 9912–9924. Curran Associates, Inc., 2020. 2, 7, 8
- [11] Mathilde Caron, Hugo Touvron, Ishan Misra, Hervé Jégou, Julien Mairal, Piotr Bojanowski, and Armand Joulin. Emerging properties in self-supervised vision transformers, 2021. 2
- [12] Ting Chen, Simon Kornblith, Mohammad Norouzi, and Geoffrey Hinton. A simple framework for contrastive learning of visual representations, 2020. 1, 2, 3, 6, 7, 8
- [13] Xinlei Chen and Kaiming He. Exploring simple siamese representation learning, 2020. 2, 6, 8
- [14] Xinlei Chen, Haoqi Fan, Ross Girshick, and Kaiming He. Improved baselines with momentum contrastive learning, 2020. 1, 2, 3, 6, 8
- [15] Xinlei Chen, Saining Xie, and Kaiming He. An empirical study of training self-supervised vision transformers, 2021. 3
- [16] Jia Deng, Wei Dong, Richard Socher, Li-Jia Li, K. Li, and Li Fei-Fei. Imagenet: A large-scale hierarchical image database. *2009 IEEE Conference on Computer Vision and Pattern Recognition*, pages 248–255, 2009. 6
- [17] Debidatta Dwibedi, Yusuf Aytar, Jonathan Tompson, Pierre Sermanet, and Andrew Zisserman. With a little help from

- my friends: Nearest-neighbor contrastive learning of visual representations, 2021. 1, 2, 8
- [18] Mark Everingham, Luc Van Gool, Christopher K. I. Williams, John Winn, and Andrew Zisserman. The pascal visual object classes (VOC) challenge. *International Journal of Computer Vision*, 88(2):303–338, 2009. 6
 - [19] Jerome Friedman, Trevor Hastie, and Robert Tibshirani. *The Elements of Statistical Learning: Data Mining, Inference, and Prediction*. Springer, New York, second edition, 2009. 7
 - [20] Spyros Gidaris, Praveer Singh, and Nikos Komodakis. Unsupervised representation learning by predicting image rotations, 2018. 2
 - [21] Jean-Bastien Grill, Florian Strub, Florent Altché, Corentin Tallec, Pierre H. Richemond, Elena Buchatskaya, Carl Dohersch, Bernardo Avila Pires, Zhaohan Daniel Guo, Mohammad Gheshlaghi Azar, Bilal Piot, Koray Kavukcuoglu, Rémi Munos, and Michal Valko. Bootstrap your own latent: A new approach to self-supervised learning, 2020. 2, 6, 7, 8
 - [22] R. Hadsell, S. Chopra, and Y. LeCun. Dimensionality reduction by learning an invariant mapping. In *2006 IEEE Computer Society Conference on Computer Vision and Pattern Recognition (CVPR'06)*, pages 1735–1742, 2006. 3
 - [23] Kaiming He, Xiangyu Zhang, Shaoqing Ren, and Jian Sun. Deep residual learning for image recognition, 2015. 6
 - [24] Kaiming He, Georgia Gkioxari, Piotr Dollár, and Ross Girshick. Mask r-cnn, 2018. 6
 - [25] Kaiming He, Haoqi Fan, Yuxin Wu, Saining Xie, and Ross Girshick. Momentum contrast for unsupervised visual representation learning, 2020. 1, 2, 3, 6, 8
 - [26] R Devon Hjelm, Alex Fedorov, Samuel Lavoie-Marchildon, Karan Grewal, Phil Bachman, Adam Trischler, and Yoshua Bengio. Learning deep representations by mutual information estimation and maximization, 2019. 2
 - [27] Ahmet Iscen, Giorgos Tolias, Yannis Avrithis, and Ondrej Chum. Mining on manifolds: Metric learning without labels. In *Proceedings of the IEEE Conference on Computer Vision and Pattern Recognition*, pages 7842–7851, 2018. 3
 - [28] Yannis Kalantidis, Mert Bulent Sariyildiz, Noe Pion, Philippe Weinzaepfel, and Diane Larlus. Hard negative mixing for contrastive learning, 2020. 2, 3, 4, 5, 6, 8
 - [29] Prannay Khosla, Piotr Teterwak, Chen Wang, Aaron Sarna, Yonglong Tian, Phillip Isola, Aaron Maschinot, Ce Liu, and Dilip Krishnan. Supervised contrastive learning, 2021. 2
 - [30] Junnan Li, Pan Zhou, Caiming Xiong, and Steven C. H. Hoi. Prototypical contrastive learning of unsupervised representations, 2021. 2, 6, 8
 - [31] Tsung-Yi Lin, Michael Maire, Serge Belongie, Lubomir Bourdev, Ross Girshick, James Hays, Pietro Perona, Deva Ramanan, C. Lawrence Zitnick, and Piotr Dollár. Microsoft coco: Common objects in context, 2015. 6
 - [32] Mohammad Mehrabi, Adel Javanmard, Ryan A. Rossi, Anup Rao, and Tung Mai. Fundamental tradeoffs in distributionally adversarial training. In *Proceedings of the 38th International Conference on Machine Learning*, pages 7544–7554. PMLR, 2021. 5
 - [33] Roy Miles and Krystian Mikolajczyk. Understanding the role of the projector in knowledge distillation, 2024. 3
 - [34] Anastasiya Mishchuk, Dmytro Mishkin, Filip Radenovic, and Jiri Matas. Working hard to know your neighbor’s margins: Local descriptor learning loss. In *Advances in Neural Information Processing Systems*, pages 4826–4837, 2017. 3
 - [35] Ishan Misra and Laurens van der Maaten. Self-supervised learning of pretext-invariant representations, 2019. 2, 3, 6, 7, 8
 - [36] Jovana Mitrovic, Brian McWilliams, Jacob Walker, Lars Buesing, and Charles Blundell. Representation learning via invariant causal mechanisms, 2020. 2
 - [37] Mehdi Noroozi and Paolo Favaro. Unsupervised learning of visual representations by solving jigsaw puzzles, 2016. 2
 - [38] Maxime Oquab, Timothée Darcet, Theo Moutakanni, Huy V. Vo, Marc Szafraniec, Vasil Khalidov, Pierre Fernandez, Daniel Haziza, Francisco Massa, Alaaeldin El-Nouby, Russell Howes, Po-Yao Huang, Hu Xu, Vasu Sharma, Shang-Wen Li, Wojciech Galuba, Mike Rabbat, Mido Assran, Nicolas Ballas, Gabriel Synnaeve, Ishan Misra, Herve Jegou, Julien Mairal, Patrick Labatut, Armand Joulin, and Piotr Bojanowski. DINOv2: Learning robust visual features without supervision, 2023. 2
 - [39] Colorado J Reed, Sean Metzger, Aravind Srinivas, Trevor Darrell, and Kurt Keutzer. Selfaugment: Automatic augmentation policies for self-supervised learning, 2021. 1
 - [40] Shaoqing Ren, Kaiming He, Ross Girshick, and Jian Sun. Faster r-cnn: Towards real-time object detection with region proposal networks, 2016. 6
 - [41] Renan A. Rojas-Gomez, Karan Singhal, Ali Etamad, Alex Bijamov, Warren R. Morningstar, and Philip Andrew Mansfield. Sssl: Enhancing self-supervised learning via neural style transfer, 2024. 1
 - [42] Chenxin Tao, Honghui Wang, Xizhou Zhu, Jiahua Dong, Shiji Song, Gao Huang, and Jifeng Dai. Exploring the equivalence of siamese self-supervised learning via a unified gradient framework, 2022. 2
 - [43] Yonglong Tian, Dilip Krishnan, and Phillip Isola. Contrastive multiview coding, 2020. 2, 3, 6
 - [44] Yonglong Tian, Chen Sun, Ben Poole, Dilip Krishnan, Cordelia Schmid, and Phillip Isola. What makes for good views for contrastive learning? In *Advances in Neural Information Processing Systems*, pages 6827–6839. Curran Associates, Inc., 2020. 1, 2, 6, 8
 - [45] Yonglong Tian, Olivier J. Henaff, and Aaron van den Oord. Divide and contrast: Self-supervised learning from uncurated data, 2021. 8
 - [46] Nenad Tomasev, Ioana Bica, Brian McWilliams, Lars Buesing, Razvan Pascanu, Charles Blundell, and Jovana Mitrovic. Pushing the limits of self-supervised resnets: Can we outperform supervised learning without labels on imagenet?, 2022. 2
 - [47] Aaron van den Oord, Yazhe Li, and Oriol Vinyals. Representation learning with contrastive predictive coding, 2019. 2, 3, 8
 - [48] Vikas Verma, Alex Lamb, Christopher Beckham, Amir Najafi, Ioannis Mitliagkas, David Lopez-Paz, and Yoshua Bengio. Manifold mixup: Better representations by interpolating hidden states. *arXiv preprint arXiv:1806.05236*, 2018. 2

- [49] Tongzhou Wang and Phillip Isola. Understanding contrastive representation learning through alignment and uniformity on the hypersphere. In *International Conference on Machine Learning*, pages 9929–9939. PMLR, 2020. 7
- [50] Xiao Wang and Guo-Jun Qi. Contrastive learning with stronger augmentations, 2022. 1, 8
- [51] Fangyun Wei, Yue Gao, Zhirong Wu, Han Hu, and Stephen Lin. Aligning pretraining for detection via object-level contrastive learning, 2021. 8
- [52] Yuxin Wu, Alexander Kirillov, Francisco Massa, Wan-Yen Lo, and Ross Girshick. Detectron2. <https://github.com/facebookresearch/detectron2>, 2019. 6
- [53] Zhirong Wu, Yuanjun Xiong, Stella Yu, and Dahua Lin. Unsupervised feature learning via non-parametric instance-level discrimination, 2018. 2, 3, 8
- [54] Tete Xiao, Colorado J Reed, Xiaolong Wang, Kurt Keutzer, and Trevor Darrell. Region similarity representation learning, 2021. 8
- [55] Enze Xie, Jian Ding, Wenhai Wang, Xiaohang Zhan, Hang Xu, Peize Sun, Zhenguo Li, and Ping Luo. Detco: Unsupervised contrastive learning for object detection, 2021. 8
- [56] Ceyuan Yang, Zhirong Wu, Bolei Zhou, and Stephen Lin. Instance localization for self-supervised detection pretraining, 2021. 8
- [57] Chun-Hsiao Yeh, Cheng-Yao Hong, Yen-Chi Hsu, Tyng-Luh Liu, Yubei Chen, and Yann LeCun. Decoupled contrastive learning, 2022. 2, 6
- [58] Sangdoo Yun, Dongyoon Han, Seong Joon Oh, Sanghyuk Chun, Junsuk Choe, and Youngjoon Yoo. Cutmix: Regularization strategy to train strong classifiers with localizable features. In *Proceedings of the IEEE/CVF International Conference on Computer Vision*, pages 6023–6032, 2019. 2
- [59] Jure Zbontar, Li Jing, Ishan Misra, Yann LeCun, and Stéphane Deny. Barlow twins: Self-supervised learning via redundancy reduction, 2021. 2, 6, 7, 8
- [60] Chaoning Zhang, Kang Zhang, Trung X. Pham, Axi Niu, Zhi-nan Qiao, Chang D. Yoo, and In So Kweon. Dual temperature helps contrastive learning without many negative samples: Towards understanding and simplifying moco, 2022. 1
- [61] Hongyi Zhang, Moustapha Cisse, Yann N Dauphin, and David Lopez-Paz. Mixup: Beyond empirical risk minimization. *arXiv preprint arXiv:1710.09412*, 2017. 2
- [62] Benjin Zhu, Junqiang Huang, Zeming Li, Xiangyu Zhang, and Jian Sun. Eqco: Equivalent rules for self-supervised contrastive learning, 2023. 2
- [63] Jiachen Zhu, Rafael M. Moraes, Serkan Karakulak, Vlad Sobol, Alfredo Canziani, and Yann LeCun. Tico: Transformation invariance and covariance contrast for self-supervised visual representation learning, 2022. 2
- [64] Chengxu Zhuang, Alex Lin Zhai, and Daniel Yamins. Local aggregation for unsupervised learning of visual embeddings, 2019. 2